

Formation mechanism of pulse current anodized film on AZ91D Mg alloy

QIAN Jian-gang(钱建刚), WANG Chun(王纯)¹, LI Di(李荻)¹,
GUO Bao-lan(郭宝兰)¹, SONG Guang-ling(宋光铃)²

1. School of Materials Science and Engineering, Beijing University of Aeronautics and Astronautics,
Beijing 100083, China;

2. CRC for Cast Metals Manufacturing, Division of Materials Engineering, School of Engineering,
University of Queensland, Brisbane, Qld 4072, Australia

Received 13 March 2007; accepted 10 May 2007

Abstract: The kinetics of forming process of pulse current anodized film on AZ91D Mg alloy was studied by the voltage—time and thickness—time curves. The surface morphology, structure, elemental constitution and valences of the anodic films were analyzed by SEM, EDS, XPS and XRD respectively. The results show that the film-forming process can be divided into four stages. Formation of a dense layer before sparking is the first stage. Formation of a porous layer accompanied with slight sparking is the second stage. The third stage is characterized by fast growth of the porous layer accompanied with more intensive sparking. The fourth stage starts after the sparking process becomes even more vigorous and the pores become large.

Key words: Mg alloy; pulse anodizing; film-forming process

1 Introduction

Magnesium alloys have an outstanding specific strength, good vibration dampening, high electric and thermal conductivities, excellent dimensional stability, good electromagnetic shielding characteristics and are easily recycled. They are regarded as environmental friendly materials of 21st century[1–3]. Unfortunately, Mg alloy has poor corrosion resistance that hinders its further application in various industrial fields. The surface treatment of Mg alloy can effectively improve its corrosion resistance and is important for widening its applied fields[4–6]. Anodizing is believed to be one of the most effective and widely used methods[7–8]. Study on direct current anodic oxidation technique at present is relatively much more extensive than that on pulsed anodic oxidation, while much attention is paid on the pulsed anodic oxidative film-forming process[9–11]. DENG et al[12] studied pulsed anodic oxidation technique by orthogonal experiments, but the film-forming process was not involved. In this work, the film-forming process of AZ91D Mg alloy was investigated by environmental friendly pulsed anodic

oxidative solution to provide theoretical guidance for further improvement of pulsed anodic oxidation technique of Mg alloy.

2 Experimental

AZ91D Mg alloy was employed in this work. The surface area of samples was 2.5 cm×3.0 cm. Before experiment, every working surface was polished successively by carborundum waterproof abrasive papers, followed by rinsing in distilled water and then acetone. They were kept in a desiccator before use.

DH1712-8 pulse electrical source was employed for pulse anodizing with a constant pulse current. The wave form of the current is shown in Fig.1. In Fig.1, I is the peak value of the current, t_1 is the anodizing time, while t_2 is the time of breaking off. Frequency $f=1/(t_1+t_2)$, duty ratio $R=t_1/(t_1+t_2) \times 100\%$.

The procedure for preparing pulse anodized film was as follows: pre-treatment→washing with tap water→pulse current anodizing→washing with tap water→drying in hot air. The major components of anodic solution were NaOH, metasilicate, borate and other

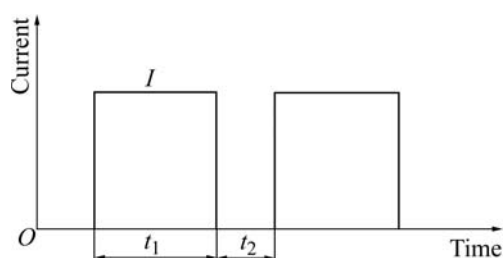


Fig.1 Scheme of wave form of current for pulse current anodizing

environmental friendly additives that contained neither Cr nor other heavy metal ions and F, P, etc[13]. The parameters of the pulse current anodizing were as follows: the duty ratio was 30%, the pulse frequency was 650 Hz, the peak value of current density was 45 mA/cm^2 and the temperature was $(15 \pm 2) \text{ }^\circ\text{C}$.

The thickness of the pulse anodic film was measured with E110B Eddy-Current Thickness Meter manufactured by the FISCHER Corp. The surface morphology, structure, composition and valence of element of the pulse anodic film were analyzed by SEM, EDS, XPS and XRD, respectively.

3 Results and discussion

3.1 Kinetic characteristic of growing anodized film

The kinetic characteristic of a growing anodized film is shown in Fig.2 and Fig.3. The growth of pulse anodized film can be divided into four stages according to the variation of voltage and the thickness of film. In Figs.2 and 3, I represents the period that both the bath voltage and thickness of film increase linearly with time, and there is no sparking at this stage; II represents the period that both the bath voltage and thickness of film increase slowly with time, and there is tiny sparking and the sparking shifts fast on the surface of Mg alloy at this

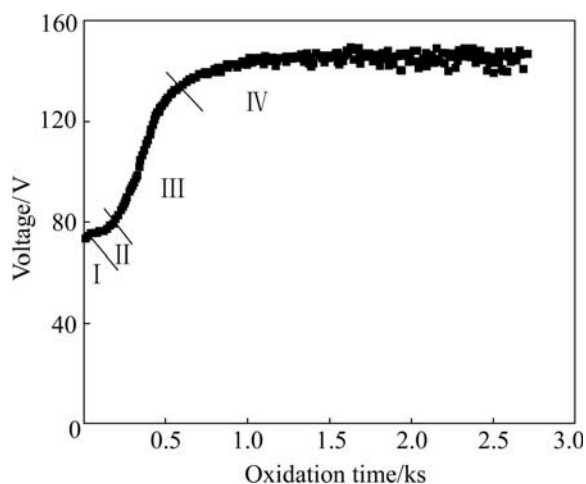


Fig.2 Voltage—time curve of pulse current anodizing

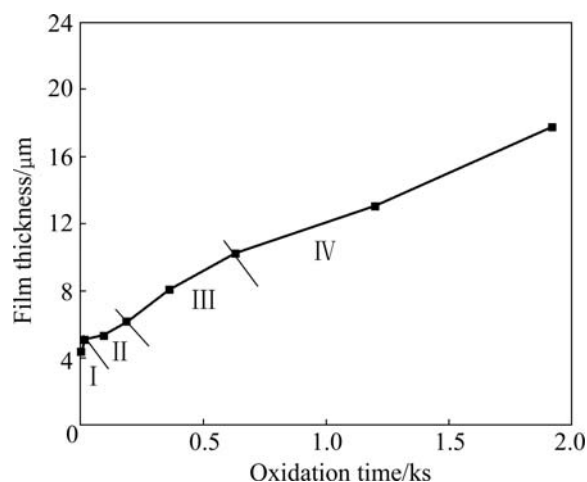


Fig.3 Thickness—time curve of pulse current anodizing

stage; III represents the period that both the bath voltage and thickness of film increase rapidly with time, and there is moderate intensity of sparking at this stage; and IV is the period that the bath voltage starts fluctuating to a certain extent while the increasing speed of film thickness reduces, and there is vigorous sparking at this stage.

3.2 Morphology, composition and structure

The variation of morphology of the pulse anodized film on AZ91D with anodizing time is shown in Fig.4. The results of analysis by EDS for the α phase (marked by A in Fig.4), β phase (marked by B in Fig.4) and the dense layer of pulse anodized film on AZ91D are listed in Table 1. The surface composition of the pulse anodized film on AZ91D is listed in Table 2. As element B cannot be detected by EDS, B isn't been counted in these tables.

The morphology of the AZ91D substrate is shown in Fig.4(a). The mark A is mainly composed of Mg, and the mark B is mainly composed of Mg and Al according to Table 1. This is in accordance with the general concept that the microstructure of AZ91D is mainly composed of α -Mg (α phase) and $\text{Mg}_{17}\text{Al}_{12}$ phase (β phase). The existence of O indicates that the surface of Mg alloy is oxidized in the air.

The morphology of film pulse anodized for 5 s (with no sparking at stage 1) is shown in Fig.4(b). As can be seen in Fig.4(b), a uniform and dense layer is formed on the surface of Mg alloy as soon as anodizing begins. The data in Table 1 denote that the content of O from both α phase and β phase increases with anodizing, which indicates that the main composition of the dense layer formed on the α phase is magnesia, and the one on the β phase is alumina.

Fig.4(c) shows that cracks occur in the dense layer formed on the α phase due to the fact that the volume

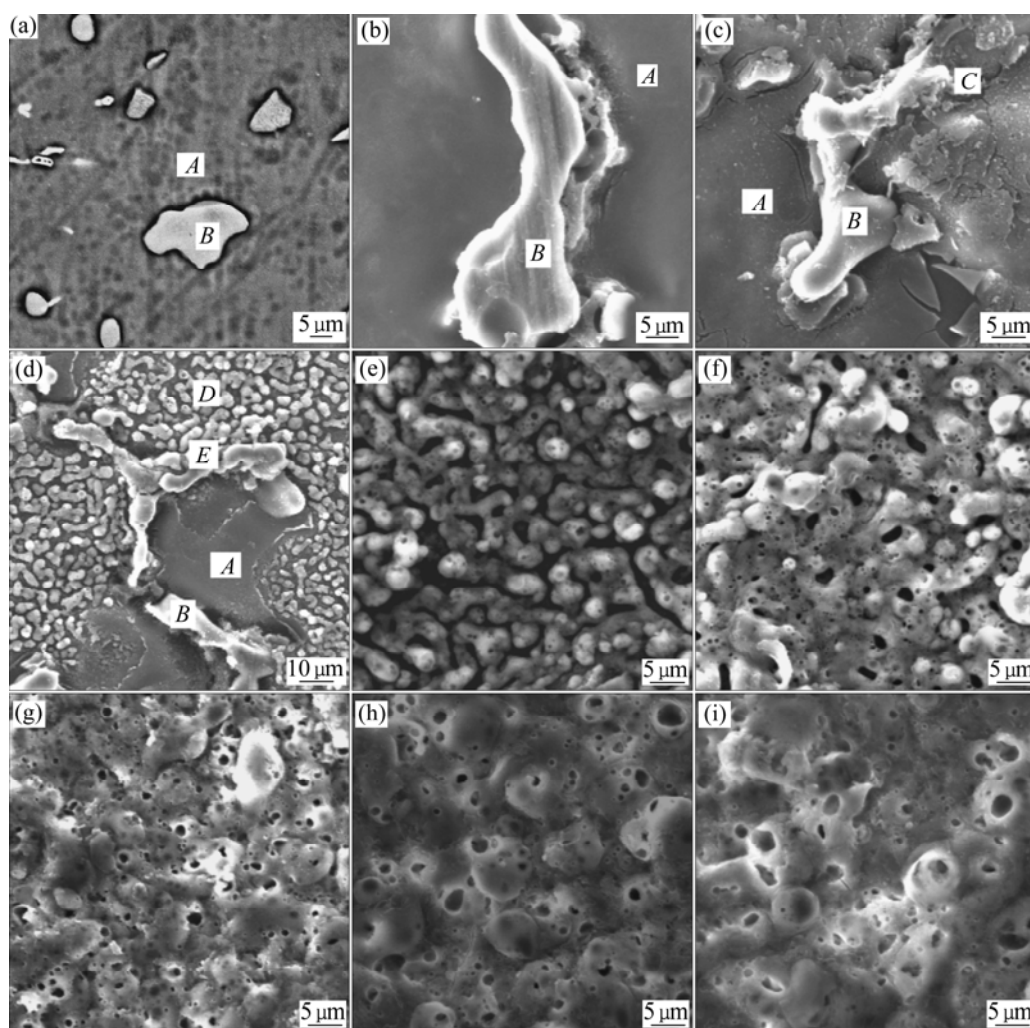


Fig.4 Surface morphologies of pulse anodized film on AZ91D at different anodizing time: (a) 0 s; (b) 5 s; (c) 16 s; (d) 95s; (e) 190 s; (f) 360 s; (g) 600 s; (h) 1 200s; (i) 1 920 s

Table 1 Composition of α phase and β phase in Fig.4 (molar fraction, %)

Oxidation time/s	O		Mg		Al		Zn		Si	
	α phase	β phase								
0	1.8	2.3	93.3	64.2	4.5	30.1	0.4	3.4	–	–
5	5.8	4.7	89.6	61.7	4.5	31.6	–	1.6	0.3	0.5
16	9.1	6.1	85.4	61.1	4.5	30.4	–	1.9	1.0	0.5
95	15.5	13.3	77.7	54.1	5.4	29.3	0.1	1.6	1.3	1.2

Table 2 Surface composition of film after pulse anodizing at different anodizing time (molar fraction, %)

Oxidation time/s	O	Mg	Al	Si	Zn	Na
5	11.4	79.2	8.4	0.9	0.1	–
16	14.9	74.8	8.5	1.5	0.3	–
95	35.3	53.2	5.8	4.8	0.9	–
190	41.6	43.8	6.0	6.9	0.8	0.7
360	50.9	31.5	4.7	9.9	–	3.0
600	52.7	28.0	3.9	11.8	–	3.6
1 200	52.3	27.5	3.8	11.9	–	4.5
1 920	53.8	25.4	3.2	11.4	–	6.2

ratio of MgO produced to Mg consumed is 0.79 when there is only MgO produced on the surface of the alloy[14]. No cracks are found on β phase. EDS analysis of the particles (mark C) reveals that the main compositions (mole fraction, %) are O 49.0, Mg 23.9, Al 18.6, Si 8.1, Zn 0.4. The contents of Si and O increase substantially at mark C as compared with the composition of the areas A, B (anodizing time is 16 s in Table 1) and the surface of AZ91D alloy before sparking. This demonstrates that sparking can accelerate the formation of compounds containing Si and O.

As can be seen more clearly in Fig.4(d), there are dense exiguous irregular particles on the surface of the alloy. EDS analysis of the particles (mark D) shows that the main compositions (mole fraction, %) are O 50.9, Mg 37.3, Al 2.3, Si 7.4 and Zn 2.1, which indicates that the irregular particles result from sparking. The elemental compositions of area E in Fig.4(d) are O 51.2, Mg 20.2, Al 13.5, Si 12.7, Zn 2.4, which indicates the same phenomenon and that the particles can be formed on both α and β phases at the same time when AZ91D is anodized. This differs from the film that formed on α phase by direct current anodizing[15]. The reason likely is that the dense layer formed on β phase with higher voltage resistance may be broken down because of the larger peak value of current density during the pulse anodic oxidation.

Fig.5 shows the detailed morphology of the particles shown in Fig.4(d). The initial structure of the film formed by sparking is porous microstructure with circular or elliptic pores.

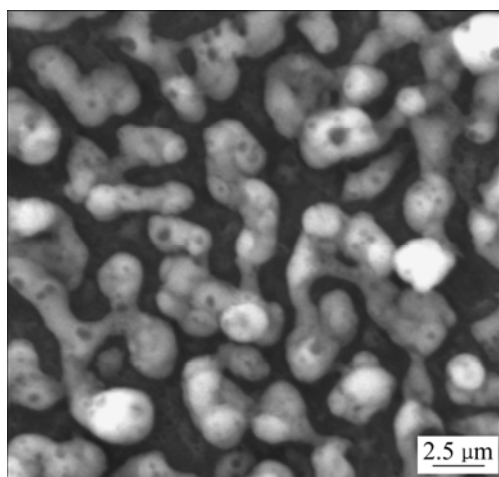


Fig.5 Detailed morphology of particles in Fig.4(d)

The number and the dimension of particles formed by sparking increase with the progress of pulse current anodizing. The gaps between particles decrease gradually until the local sections of sparking product are connected each other which cover the whole surface of the alloy

(shown in Fig.4(e)). With regard to the composition of the film, the contents of Si and O increase, while those of Mg and Al decrease. At this stage, the pore size of the sparking products is almost unchanged as the variation of sparking is small.

The porous layer starts to grow and overlaps as pulse current anodizing continues. The morphology of the film pulse current anodized for 6 min is shown in Fig.4(f). As can be seen, there are two kinds of pores in the film. One is relatively small in shape of circular or ellipse which is similar with the pore of sparking product in Fig.5. The other is relatively large in irregular shape and is located at the boundary of particulate structure.

Consequently, it can be concluded that there are two kinds of pores in the pulse current anodized film on Mg alloy. The first group of pores is in shape of circular or ellipse possessed by sparking product which becomes larger with sparking and is defined as the first kind of pores. The second group of pores is the gaps resulted from connection of the sparking products, which is in irregular shape and correlates to the growth and connection of the sparking products as well as overlapping of the porous film and is defined as the second kind of pores. As the gaps decrease with anodizing time, the second kind of pores can diminish gradually.

After 10 min of anodizing (shown in Fig.4(g)), the second kind of pores disappear essentially due to the porous film overlapping and the film thickness increasing. Meanwhile, the first kind of pores increase with anodizing time.

When pulse current anodizing is carried on, the thickness of film keeps increasing and the sparking becomes more and more intensive, then the first kind of pores expands continuously, as shown in Figs.4(h) and (i). The data in Table 2 denote that the composition of the pulse current anodized film is approximately unchanged.

Further analysis of the pulse current anodized film by XPS indicates that there exist O^{2-} , Mg^{2+} , Si^{4+} , B^{3+} , Al^{3+} and Na^+ in the anodized film whose electron binding energies are 531.1, 50.4, 102.2, 192.4, 73.7 and 1 070.6 eV, respectively. Compared with EDS, the XPS results show that there is a new element of B in the anodized film, in addition to O^{2-} , Mg^{2+} , Si^{4+} , B^{3+} , Na^+ and Al^{3+} . The Na^+ results from adsorption. The larger the pores are, the more the Na^+ ions are adsorbed.

The XRD results of the 10 min anodized film are shown in Fig.6. As can be seen, the pulse current anodized film is mainly composed of MgO, $Mg_3B_2O_6$ and Mg_2SiO_4 . The content of Al^{3+} in the film is too little to be detected by XRD.

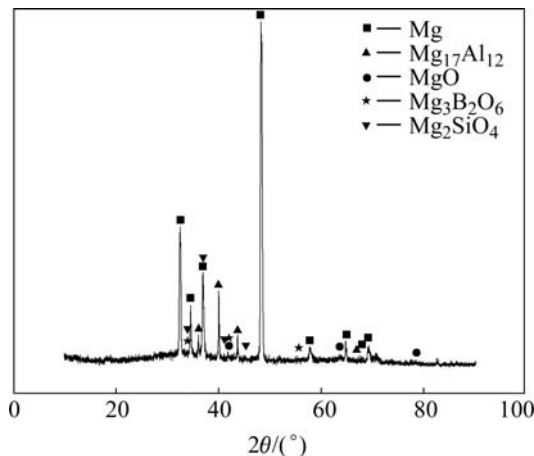


Fig.6 XRD pattern of pulse anodized film on AZ91D

4 Conclusions

1) The forming process of pulse current anodized film on AZ91D Mg alloy can be divided into four stages according to the characteristic of voltage, thickness, morphology, composition and constitution of the anodized film in growth: formation of dense layer, formation of porous layer, fast growth of the porous layer and slow growth of the porous layer.

2) At the first stage, different oxides are formed on α phase and β phase respectively. There are micro-cracks on partial area of the α phase film, while the film grown on the β phase is intact.

3) At the second stage, sparking starts to occur on the dense layer and porous sparking products are formed. As anodizing goes on, the sparking products increase in number and dimension and extend to connect with each other until cover the whole surface of the Mg alloy, and thereafter, a porous layer is formed on the dense layer. There are two kinds of pores in the film. The first kind forms in sparking product itself, which is in circular or elliptic. The second kind is from irregular gap resulting from connection of the sparking products.

4) At the third stage, the porous layer starts to overlap. The thickness of the anodized film increases substantially. The second kind of pores becomes smaller with the increase of porous film thickness. The first kind of pores enlarges at this stage.

5) At the fourth stage, the porous layer grows slowly,

and the composition of the porous layer is almost unchanged. The first kind of pores becomes larger and larger.

References

- [1] RUDEN T J, ALBRIGHT D L. High ductility magnesium alloys in automotive applications [J]. *Advanced Material & Processes*, 1994, 145(6): 28–32.
- [2] FROES F H, LIEZER D. The science, technology and application of magnesium [J]. *J Mine Metals and Mater Soc*, 1998, 5(9): 30–34.
- [3] QIAN Jian-gang, LI Di, GUO Bao-lan. Surface treatment of magnesium alloy [J]. *The Chinese Journal of Nonferrous Metals*, 2002, 12(3): 32–36. (in Chinese)
- [4] BARTON T F, JOHNSON C B. Anodization of magnesium and magnesium based alloys [J]. *Plating Surface Finishing*, 1995, 82(5): 138–141.
- [5] ZOZULIN A J, BARTAK D E. Anodized coatings for magnesium alloys [J]. *Metal Finishing*, 1994, 92(3): 39–43.
- [6] NAKATSUGAWA T, MARTIN R, KNYSTAUTAS E J. Improving corrosion resistant of AZ91D magnesium alloy by nitrogen ion implantation [J]. *Corrosion*, 1996, 52(12): 921–926.
- [7] SONG Guang-ling. Recent progress in corrosion and protection of magnesium alloys—An overview of cast's research work [J]. *Advanced Engineering Materials*, 2005, 7(7): 563–586.
- [8] SONG Guang-ling. Corrosion and protection of magnesium alloys—An overview of research undertaken by cast [J]. *Materials Science Forum*, 2005, 488/489: 649–652.
- [9] ZHANG Yong-jun, YAN Chuan-wei, WANG Fu-hui, LOU Han-yi, CAO Chu-nan. Study on the environmentally friendly anodizing of AZ91D magnesium alloy [J]. *Surface and Coatings Technology*, 2002, 161: 36–43.
- [10] KHASELEV O, YAHALOM J. The anodic behaviour of binary Mg-Al alloys in KOH-aluminate solutions [J]. *Corrosion Science*, 1998, 40(7): 1149–1160.
- [11] HSIAO H Y, TSAI W T. Characterization of anodic films formed on AZ91D magnesium alloy [J]. *Surface and Coatings Technology*, 2005, 190: 299–308.
- [12] DENG Shu-hao, YI Dan-qing, LOU Jia. Pulsed anodizing process of magnesium alloys [J]. *Electroplating & Finishing*, 2006, 25(2): 32–35.
- [13] QIAN Jian-gang, LI Di, GUO Bao-lan. The study of environment-friendly processes of the anodization for magnesium alloys [J]. *Journal of Aeronautical Materials*, 2003, 23(10): 109–112.
- [14] WANG He-nan, HUO Hong-wei, LI Ying. The new technology of the anodic oxidation applied to AZ91D alloy [J]. *Journal of Chinese Society for Corrosion and Protection*, 2003, 23(5): 286–289.
- [15] QIAN Jian-gang, LI Di, ZHANG Feng. Process of film formation by anodizing AZ91D magnesium alloy [J]. *Materials Science Forum*, 2005, 475/479: 3905–3908.

(Edited by LI Xiang-qun)